Full Paper Transactions, SMiRT 28
Toronto, Canada, August 10-15, 2025

Seismic Fragility Evaluation of a Thin-Walled Vessel in a Sodium-Cooled Fast Reactor

Tomoyoshi Watakabe[1], Hidemasa Yamano[2], Satoshi Futagami[3]

[1] Principal Researcher, Japan Atomic Energy Agency, Ibaraki, JAPAN (watakabe.tomoyoshi@jaea.go.jp)
[2] Deputy Director, Japan Atomic Energy Agency, Ibaraki, JAPAN
[3]Group Leader, Japan Atomic Energy Agency, Ibaraki, JAPAN

INTRODUCTION

A sodium-cooled fast reactor (SFR) has been developed as one of the options to contribute to decarbonization in Japan in 2050. Japan has experienced disasters due to huge earthquakes. To enhance nuclear safety, it is important to see the failure risk of passive components in the SFR under an excessive earthquake in advance. Past studies showed that buckling of a reactor vessel (RV) mainly contributes to the seismic core damage frequency (CDF) in the SFR [Naruto et al., 2014]. It is necessary to investigate the seismic response and fragility of the RV important to safety in the SFR under seismic loading.

The RV in the SFR is composed of a thin-walled cylinder. As a component with a thin-walled cylinder, there are steel storage tanks above ground used in general industrial facilities. The seismic response and fragility of the storage tank have been studied in past studies [Phan et al., 2016]. However, the storage tank has a thinner wall thickness than the RV of the SFR. Also, the dynamic analysis must consider the uplift phenomenon because a base is not anchored to the ground. In addition, there is also a difference in earthquake conditions: RV is subjected to the response wave at the located floor of the reactor building, while the storage tank is directly subjected to ground earthquake. Therefore, this study has investigated the seismic response and fragility considering the structural features of the RV and input conditions in the SFR.

The RV in the SFR used under a high-temperature condition results in a thin-walled structure because of the mitigation of thermal stress. In the structural design of the RV in the SFR, the structural integrity has been evaluated by preventing the occurrence of buckling [JSME, 2018]. Fragility on the RV was evaluated to assume that the failure mode was buckling, which is used in the design, so far. However, it is considered that the vessel maintains the boundary of cooling material even after buckling [Ogiso et al., 1996] and does not lose the function of maintaining the RV coolant level. The RV is cyclically subjected to post-buckling seismic load, which would finally result in the fatigue failure of the RV (leak of coolant). To evaluate the practical fragility of the RV, in this study, it is adequate that fatigue is defined as failure mode, not buckling.

The fragility evaluation method of the RV in the SFR has been developed for both failure mode buckling and fatigue [Yamano et al., 2019; Nishino et al., 2024]. These studies showed the fragility using the RV of a loop-type SFR: radius R / thickness t is about 100 [Nishino et al., 2024]. Recently, Japan Atomic Energy Agency (JAEA) together with Japanese industrial partners has been conducting a pool-type SFR design [Uchita et al., 2021]. The fragility of the pool-type RV has never been evaluated by the proposed method, which is based on the fatigue failure mode instead of the buckling. To investigate the basic behaviour of the pool-type RV under excessive seismic loading, this report investigated the fragility by using a simple cylindrical model with a wall thickness close to the design of the pool-type RV: R/t is 200, as the first trial.

FRAGILITY EVALUATION MODEL AND CONDITIONS

This study provides the fragility evaluation results of two cases using a thin-walled cylindrical vessel model (R/t=200). One is fatigue-based fragility, which is the case assuming that the vessel loses integrity due to fatigue failure. The other is buckling-based fragility, which is the case assuming that the vessel loses integrity due to the occurrence of buckling.

Analysis Model

A series of buckling tests for the SFR's RV was conducted to investigate buckling loads and modes in the past studies [Matsuura et al., 1987]. The test was carried out by using the specimen, focusing only the cylindrical part, where significant stress occurred in the evaluation of RV integrity. The specimen consists of a type 304 stainless steel vessel and a rigid cylinder. The specimen dimensions were scaled down, but R/t corresponds to that of the practical RV. The ratio of the radius (500mm) of the vessel and the thickness (2.5mm) R/t is 200, which is slightly larger than that of the pool-type RV in the current design: R/t is 160. The rigid cylinder, of which wall thickness is 10 times larger than that in the vessel part, was set up on the specimen to fit the height of the test apparatus in the test-specific circumstances. The top of the specimen was loaded by an actuator in a horizontal direction to investigate the static performance of the vessel. This study selected the specimen as the analysis subject because it is considered that the specimen incorporates major characteristics of the RV. Figure 1 shows the analysis model that was prepared for this study.

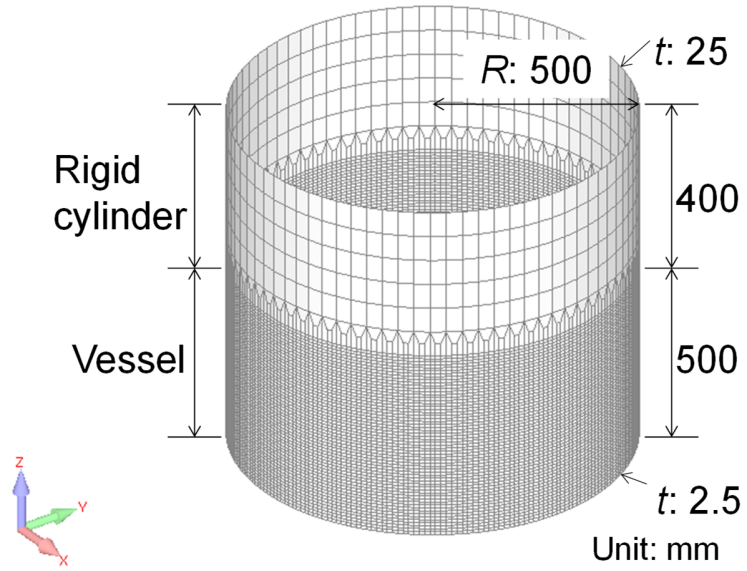

Figure 1. Analysis model

Simulation of Test

We carried out a simulation using the analysis model and compared it to the test result to validate the analysis model. FINAS/STAR version 2020 [ITOCHU Techno-Solutions Corporation, 2020], a finite element analysis (FEA) code, was used for the analysis in this study. The analysis model mainly consisted of 4-nodes MITC (Mixed Interpolation of Tensorial Components) shell elements named as Quad4. The element mesh of the vessel part was divided into 240 elements along the hoop direction and 60 elements along the axial direction. Figure 2 shows the material property at 350℃ used in the analysis. Plasticity of

the material was expressed by both multilinear and bi-linear with isotropic hardening rule. The rigid cylinder was also expressed by Quad4. The element mesh of the rigid cylinder was divided into a coarse mesh to reduce calculation time: 80 elements along the hoop direction and 6 elements along the axial direction. Static displacement was added to the positive x-direction under the loading to the axial z-direction to cancel the weight of the rigid part.

Figure 3 shows a comparison between the test result and the analysis results on the load-displacement curve at the top of the model. The analysis with multi-linear evaluated a larger maximum load than the test result by approximately 1%. The analysis result with multi-linear was in good agreement with the test result. There is some difference of behaviour between the analysis result of bi-linear and the test result around the maximum load. This is attributed that bi-linear has a higher yield stress than the real material property. However, the error ratio of the maximum load was approximately 8% at most. Figure 4 shows the equivalent plastic strain contour of multi-linear and bi-linear in the maximum displacement of analysis results, 3.4mm. Strain contour and buckling deformation are comparable between multi-linear and bi-linear as shown in Figure 4, and the maximum equivalent plastic strain was 0.041 in multi-linear and 0.046 in bi-linear. From the results, it was confirmed that the analysis model was adequate to evaluate the response of the vessel.

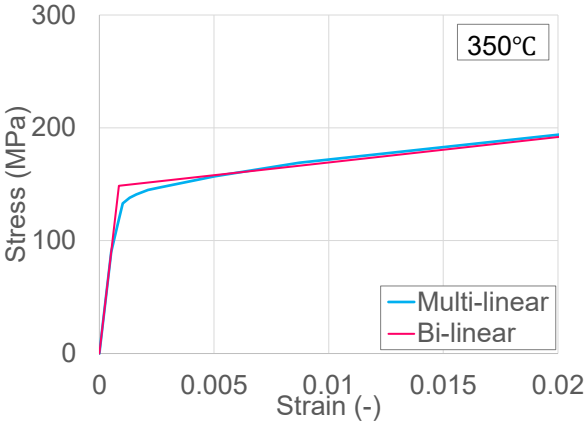

Figure 2. Stress-strain curve of 304-type stainless steel for simulation of the static test

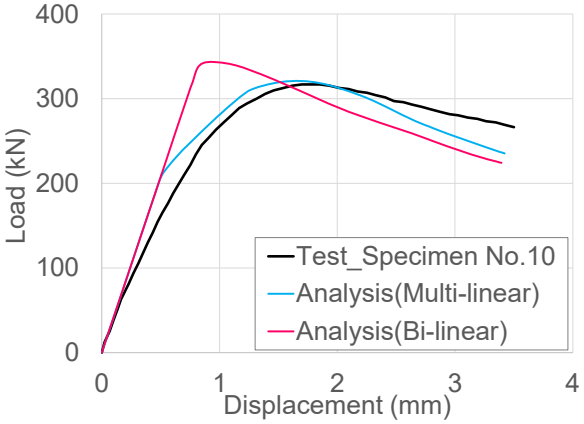

Figure 3. Comparison between the test and the analysis on the load-displacement curve

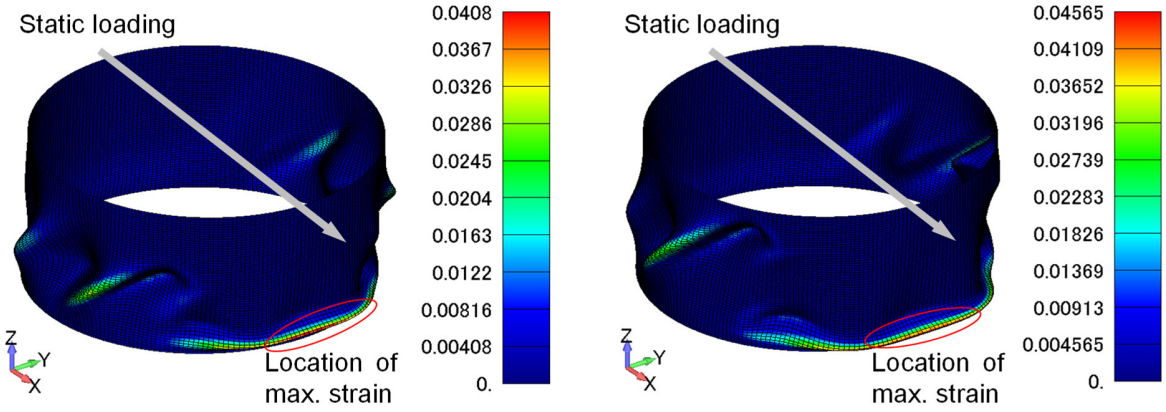

(a) Multi-linear (b) Bi-linear

Figure 4. Equivalent plastic strain contour of multi-linear and bi-linear in maximum displacement of analysis results, 3.4mm

Dynamic Analysis Conditions

We conducted time history analyses to estimate each input level's dynamic response by using the analysis model. FINAS/STAR version 2020 was also used for the analysis. The following conditions were additionally assumed in the analysis. Total added masses of 472.8ton in the horizontal direction and 605.2ton in the vertical direction were distributed to each node of the top end along the hoop direction evenly so that the natural frequency of the model corresponds to those of the practical vessel in the SFR, 4Hz in the horizontal direction and 10Hz in the vertical direction. The stiffness proportional type damping for 5% was applied in the analysis. Figure 5 shows the material property used in the analysis. The stress-strain curve provided in the fast reactor (FR) code issued by Japan Society of Mechanical Engineers (JSME) was used to extend to strain 0.2 [JSME, 2018] because it is necessary to simulate the vessel response with a larger strain beyond a design level in the fragility evaluation. In the analysis for fatigue-based fragility, plasticity was expressed by the bi-linear in Figure 5 and Table 1. Meanwhile, elasticity was assumed in the analysis for buckling-based fragility. This is because the integrity against buckling was evaluated based on the design method using elastic analysis as described in the following section, buckling evaluation.

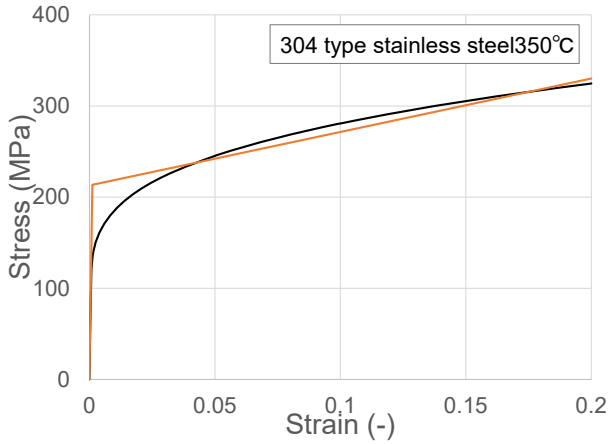

Figure 5. Comparison between stress-strain curve of 304 type stainless steel on JSME FR code and bi-linear model for the analysis

Table 1: Material property set in the analysis

Elastic modulus	MPa	174000
Density	[ton/mm^3]	7.89×10^{-9}
Poisson's ratio	[-]	0.28
Initial yield stress	MPa	213.5
Secondary hardening coefficient	MPa	583.4

The reactor building of the SFR plans to employ a seismic isolation system, as shown in Figure 6. The floor response wave (Figure 7) at the location of the RV was used as the input to the analysis model, which includes the characteristics of the building with a horizontal seismic isolation system subjected to design earthquake [Uchita et al., 2021]. The peaks of the spectrum are seen at the longer period range of around 3s in the horizontal wave and the higher frequency range of around 7Hz in the vertical wave. Three

directional waves, North-South (NS), East-West (EW), and Up-Down (UD), were simultaneously input at the bottom of the analysis model. Both characteristics of the two horizontal waves, NS and EW, were mostly comparable. It is necessary for the fragility evaluation of the RV to perform step-by-step analyses in each input level up to failure. The seismic input of the practical plant was severe for the analysis model, which was scaled down. Therefore, the input wave was multiplied by 0.17 times, which was determined as the reference wave in the analysis.

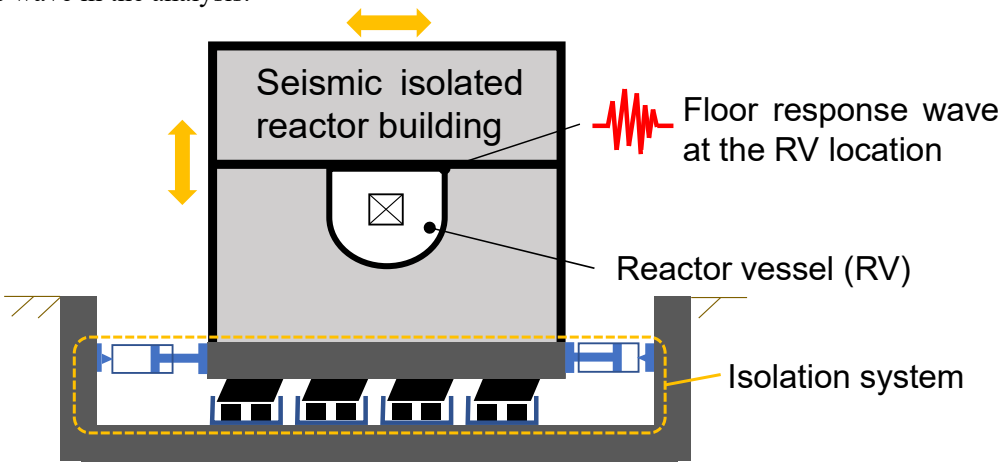

Figure 6. Schematic of the SFR with horizontal isolation system

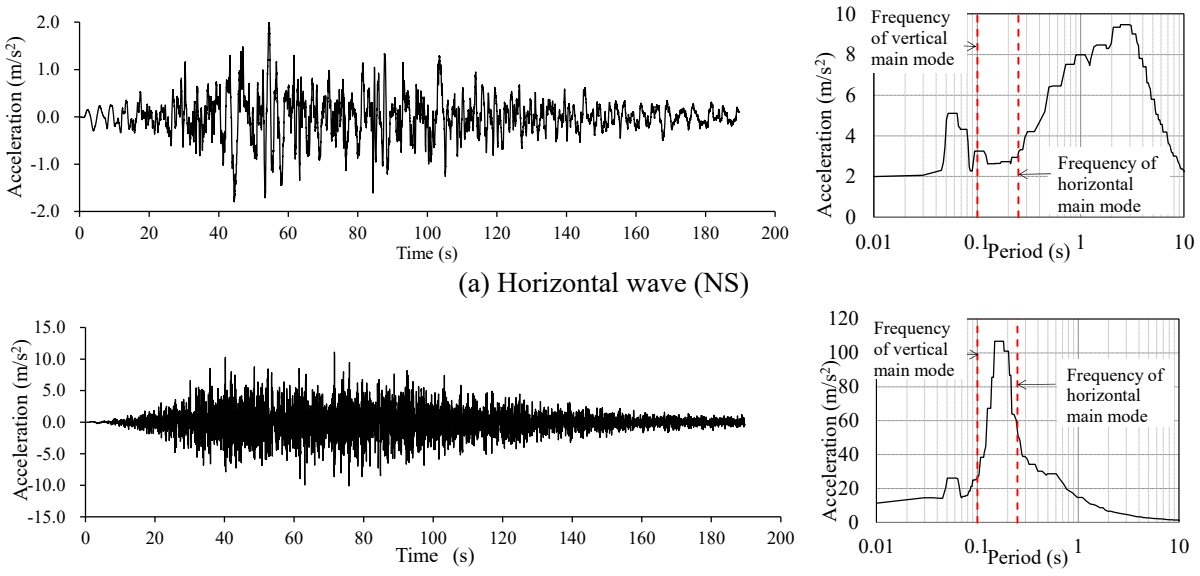

(a) Horizontal wave (NS)

(b) Vertical wave (UD)

Figure 7. Time history and response spectrum of seismic input for the analysis

Fatigue-based fragility evaluation

Fatigue integrity was evaluated by referring to the method of JSME code case, which provides for a reasonable piping design method based on inelastic analysis and strain-based criteria [JSME, 2019]. This method was applied to the evaluation of the fatigue fragility of the RV as follows.

Step 1: The dynamic inelastic FEA estimates the dynamic response of the vessel, and the local strain components at the model's mesh where the cumulative plastic strain was the largest were extracted from the analysis results.
Step 2: The extrema in the time history of the representative strain components among all strain components were counted by the rain flow method. Then, the equivalent strain was calculated using all strain components in each time occurrence.
Step 3: The usage factor was calculated based on the miner's rule from the relationship between the strain histogram counted in Step 2 and the average fatigue curve of the material as shown in Figure 8 [JSME, 2018]. The RV was judged as fatigue failure when the usage factor reached unity.
Step 4: The fragility was evaluated using the safety factor method shown in Equation 1 [AESJ, 2015]. The response factor of a reactor building includes the effectiveness due to the nonlinearity of the seismic isolation system, which is estimated by the regression line of the relationship between input acceleration to the building and the floor response at the RV location [Nishino et al., 2024]. The capacity factor was determined to consider not including the safety margin due to the allowable limit and fatigue curve in the above fatigue evaluation procedure.

$$F(A) = \Phi\left[\frac{\ln(A/(F_C \cdot F_R \cdot A)) + \Phi^{-1}(p) \cdot \beta_u}{\beta_r}\right] \quad (1)$$

where $F(A)$ is the fragility for a seismic acceleration input to building A, A is the seismic acceleration input to building for the basis earthquake, F_C is the capacity factor of components, F_R is the response factor of the building and components, β_r is the logarithmic standard deviation which expresses aleatory uncertainty, β_u is the logarithmic standard deviation which expresses epistemic uncertainty, Φ is the standard normal probability distribution function, and p is the confidence level determined by the non-exceedance probability considering the epistemic uncertainty.

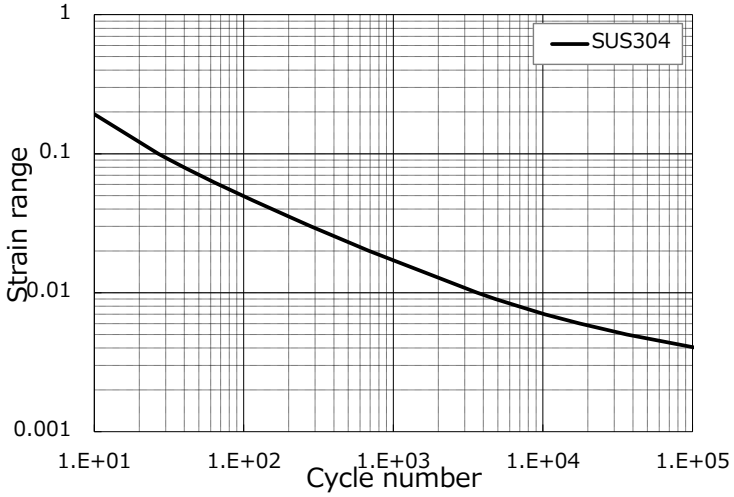

Figure 8. Average fatigue curve used for fatigue evaluation [JSME, 2018].

Buckling-based fragility evaluation

Buckling integrity was evaluated based on the design method using an elastic response and Equation 2 based on the five power laws that have been developed for the design of the vessel in the SFR [Okafuji et al., 2021].

$$\left(\frac{Q}{Q_{cr}}\right)^5 + \left(\frac{M}{M_{cr}} + \frac{F}{C_v F_{cr}}\right)^5 \leq \left(\frac{1}{f_B}\right)^5 \quad (2)$$

where Q/Q_{cr} is the ratio of the shear force to the shear buckling strength, M/M_{cr} is the ratio of the bending moment to the bending moment strength, F/F_{cr} is the axial compression force to the axial buckling strength, C_v is the correlation factor to consider the reduction effect of the buckling strength by cyclic axial loading under horizontal base isolation, and f_B is the design factor. Buckling-based fragility of the RV was evaluated as the following steps.

Step1: The maximum reaction forces of the vessel, bending moment, shear force, and axial force, were estimated by the dynamic elastic FEA. The used analysis model is common with that of the fatigue evaluation, but the material property was assumed to be elasticity.
Step2: The occurrence of buckling was evaluated to substitute each reaction force obtained by the analysis results in Step1 into Equation 2.
Step3: Fragility was evaluated using the safety factor method. The response factor of a reactor building was determined as the same as fatigue-based fragility one. The capacity factor was determined to consider the safety margin including in allowable limit and calculation process of the response in the buckling evaluation.

EVALUATION RESULTS

Dynamic behaviour

Figure 9 shows the deformation and equivalent plastic contour of the vessel under 1.3 times the input of the reference wave. The elephant foot buckling appeared first at the lower fixed point in the early time around 50s. After that, as the horizontal response becomes larger, shear buckling appears at the side of the cylinder. Complex buckling deformation due to the superposition of axial load and shear load was seen, and the strain concentration was observed at the round cylinder of the lower position close to the fixed. From the result of the top view, it was confirmed that the significant horizontal deformation of the vessel was observed at the middle degrees of x-axis and y-axis. This is because a maximum inertial load occurs at the middle degrees of x-axis and y-axis in case of two horizontal direction excitations using two same waves.

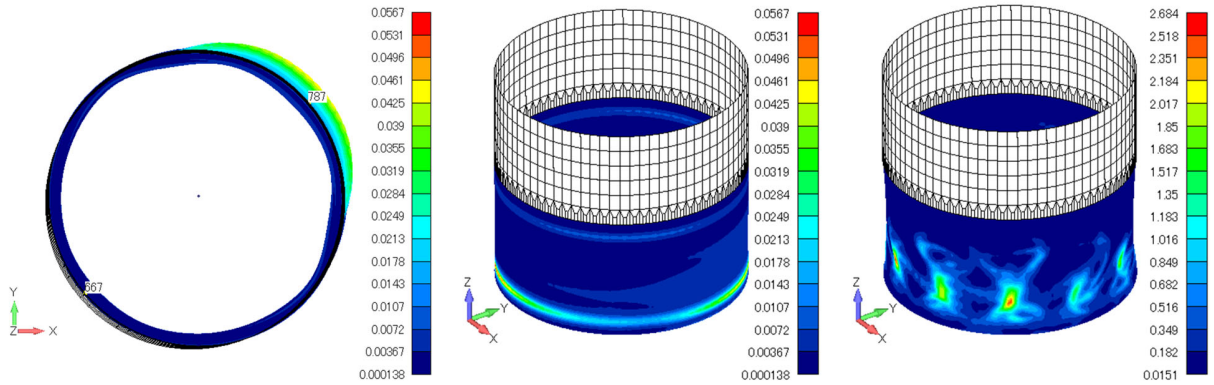

(a) Top view (50s) (b) Side view (50s) (c) Side view (90s)
Figure 9. Equivalent plastic contour with deformation (1.3 times the input of the reference wave)

Table 2 shows buckling evaluation results on the reference wave. From the results, axial force was the most critical force in light of buckling of the vessel. It can be seen that shear force also occurs, which has the second highest impact on buckling of the vessel. The results explain that elephant foot buckling due to axial

force occurs first in time duration, and shear buckling due to shear force occurs next. In case of horizontal isolation plant, it is considered that the axial force is severe in the vessel, because the vertical load is basically larger than the horizontal load, as shown in the spectrum of Figure 6. This tendency would change depending on the dimension of the vessel, loading height, and so on; therefore, more analytical study is necessary.

Table 2: Buckling evaluation results on the reference wave

Model	Shear force	Bending moment	Axial force	Total	Limit
R/t	Q/Q_{cr}	M/M_{cr}	F/C_vF_{cr}	$((Q/Q_{cr})^5+(M/M_{cr}+F/C_vF_{cr})^5)^{1/5}$	$1/f_B$
200	0.757	0.001	1.392	1.395	1

Fragility curve

It is considered that the loss of function of the vessel is practically caused by the leak of coolant due to fatigue failure. The fatigue-based fragility curve in the thin-walled vessel with R/t of 200 was calculated, which is compared to the buckling-based fragility curve in this study. Figure 10 shows the fatigue-based fragility curve and the buckling-based fragility curve. If we see the multiplier to the reference wave corresponding to the failure probability 0.5 (after this median acceleration), these are 0.9 in the buckling-based and 1.8 in the fatigue-based. The fatigue-based result is approximately twice as large as the buckling-based result. The results indicated that the fatigue-based method could reasonably evaluate the failure risk even in the thin-walled vessel with R/t of 200, which is larger than that of the pool-type SFR vessel shape.

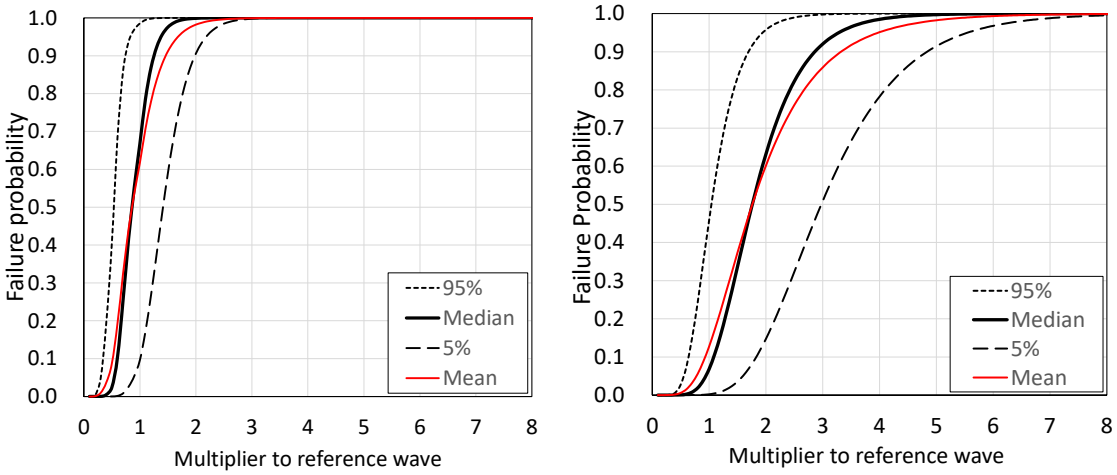

(a) Buckling-based (b) Fatigue-based

Figure 10. Fragility curve

CONCLUSION

This paper described the fragility evaluation results of the cylindrical vessel model (R/t=200), which is larger than that of the pool-type SFR vessel (R/t=160). The dynamic behaviour of the vessel up to ultimate strength was investigated through the dynamic nonlinear FEA under an excessive earthquake. From the result, it was confirmed that the vessel finally reached fatigue failure at the cylindrical part where strain concentration was significant accompanying the large deformation due to elephant foot buckling and shear

buckling. In addition, the fragility curve was provided in case of buckling and fatigue are assumed as failure modes. It was confirmed that the fatigue-based method reasonably evaluated the fragility, which was twice as large as the buckling-based fragility. This tendency was comparable to that of the loop-type SFR vessel, which was confirmed in the past study. The fragility evaluation based on the fatigue failure mode after buckling would be applied to the pool-type SFR design in the future.

ACKNOWLEDGMENTS

The present paper includes the results of "Technical development program on a fast reactor for demonstration, Program Grant Number JPMT007143" and "The Program to Support the Development of Innovative Nuclear Power Technologies in Response to Society's Needs" entrusted to Japan Atomic Energy Agency by Ministry of Economy, Trade and Industry in Japan. The authors are grateful to C. Jin, S. Sugaya, T. Kodama, W. Gu, S. Suzuki, and Y. Nanazawa, ITOCHU Techno-Solutions Corporation (CTC), for their contributions. The authors appreciate to K. Abe, Tokokikaikogyo Corporation, for supporting a series of analyses.

REFERENCES

Atomic Energy Society of Japan. (2015). *A standard for Procedure of Seismic Probabilistic Risk Assessment for Nuclear Power Plants*, AESJ-SC-P006E: 2015.

ITOCHU Techno-Solutions Corporation. (2020). FINAS/STAR Version 2020, Theoretical manual (in Japanese).

Japan Society of Mechanical Engineers. (2018). *Codes for Nuclear Power Generation Facilities, Rules on Design and Construction for Nuclear Power Plants*, *Section II Fast Reactor Codes*, JSME S NC2-2018 (in Japanese).

Japan Society of Mechanical Engineers. (2019), *An Alternative Rules on Seismic Design of Seismic S Class Piping by Elastic-Plastic Response Analysis*, JSME NC-CC-008 (in Japanese).

Matsuura, S., Nakamura, H., Kobayashi, S., Sakurai, A. (1987). "Buckling Strength of Main Vessel of LMFBR under Transverse Shearing Load," *Reports of Central Research Institute of Electric Power Industry* (in Japanese).

Naruto, K., Nishino, H., Kurisaka, K., Yamano, H., Okano, Y., Okamura, S., Eto, M. (2014). "Seismic PRA for Japan sodium-cooled fast reactor (JSFR)," *Proceedings of the 9th Korea-Japan Symposium on Nuclear Thermal Hydraulics and Safety (NTHAS9)*, Buyeo, Korea, No.9A0017.

Nishino, H., Kurisaka, K., Futagami, S., Watakabe, T., Yamano, H. (2024). "Effectiveness Evaluation of the Measures for Improving Resilience of Nuclear Structures against Excessive Earthquake (1) Fragility Evaluation of Reactor Vessel based on Structural Analysis," *Proceedings of the 17th International Conference on Probabilistic Safety Assessment and Management and Asian Symposium on Risk Assessment and Management (PSAM17&ASRAM2024)*, Sendai, Miyagi, Japan.

Ogiso, S., Sasaki, T., Oooka, Y., Nakamura, H., Matuura, S., Akiyama, H. (1996). "Seismic Buckling Design Guideline of FBR Main Vessels (6th Report, Postbuckling Fatigue Damage Evaluation on FBR Main Vessels)," *Transactions of the Japan Society of Mechanical Engineers*, Part A, 62, 598, pp.1306-1315, (in Japanese).

Okafuji, T., Miura, K., Sago, H., Murakami, H., Ando, M., Miyazaki, M. (2021). "Development of the Buckling Evaluation Method for Large Scale Vessel by the Testing of GR. 91 Vessel Subjected to Horizontal and Cyclic Vertical Loading," *Proceedings of the ASME 2021 Pressure Vessels and Piping Conference*, Virtual conference *(PVP2021)*, PVP2021-60672.

Phan, H., N., Paolacci, F., Alessandri, S. (2016). "Fragility Analysis Methods for Steel Storage Tanks in Seismic Prone Areas," *Proceedings of the ASME 2016 Pressure Vessels and Piping Conference*, Virtual conference *(PVP2016)*, PVP2016-63102.

Uchita, M., Miyagawa, T., Murakami, H., Suzuno, T., Yamamoto, T. (2021). "A Study on Structures of Reactor Vessel of Pool-type Sodium-cooled Fast Reactor in case of adopted Three-Dimensional Isolation System," *Transactions of 2021 Fall meeting in the Atomic Energy Society of Japan*, (in Japanese).

Yamano, H., Nishida, A., Choi, B., Takada, T. (2019). "Development of Seismic Counter Measures against Clif Edges for Enhancement of Comprehensive Safety of Nuclear Power Plants Part 10: Avoidance of Clif Edge for Reactor Vessel," *Transactions of the 25th International Conference on Structural Mechanics in Reactor Technology (SMiRT-25)*, Charlotte, NC, USA.